

INTERNAL MEMORANDUM

February 15, 2006

To: R. Gredel - Chair
Cc: ELT Site Evaluation Working Group
From: F. Patat - USD

Subject: Impact of optical and near-IR Sky brightness on Site Evaluation

1 Introduction

The presence of an emission background from the Earth's atmosphere is a transversal problem in the context of site evaluation, in the sense that it affects all instruments which operate in background-limited conditions. Of course the impact changes according to the different wavelength ranges covered and so does the dominating physical mechanism which is responsible for the radiation emission.

The night sky light as seen from ground is generated by two classes of sources:

- extra-terrestrial (unresolved stars/galaxies, diffuse galactic background, zodiacal light);
- terrestrial (airglow, auroral activity and thermal emission);

While the extra-terrestrial components vary only with the position on the sky and are therefore predictable, the terrestrial ones are known to depend on a large number of parameters (season, geographical position, solar cycle and so on) which interact in a largely unpredictable way. In fact, airglow contributes with a significant fraction to the global night sky emission and hence its variations have a strong effect on the overall brightness.

In this document I will discuss mostly the terrestrial component, since this may depend on the site location and, therefore, it has to be considered among the parameters that characterize a given site. We will also briefly mention the extra-terrestrial component, since the site latitude is directly related to the sky region covered by the observations and hence to the typical extra-terrestrial background (zodiacal light, galactic background).

An overview of the contributions by different sources to the sky brightness is given in Fig. 1.

2 Natural terrestrial components

The terrestrial component can be subdivided into two distinct phenomena, i.e. airglow and aurorae. The main emission features are summarized in Tab. 1 for the two classes, while spectra extending from $0.34 \mu m$ to $5 \mu m$ are presented in Figs. 2 and 3.

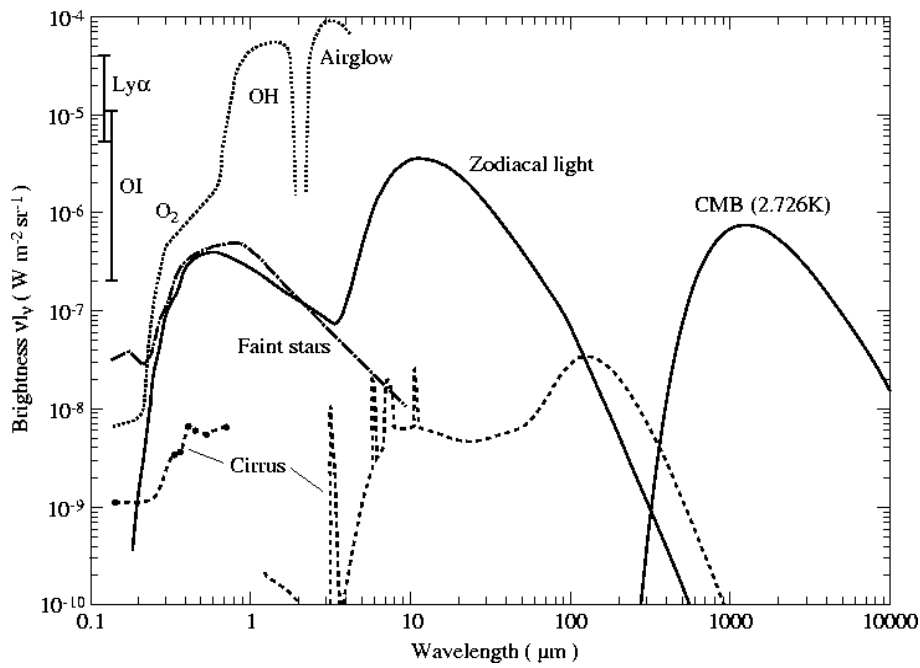


Figure 1: Overview of the night sky brightness outside of the lower terrestrial atmosphere and at high ecliptic latitudes (from [11]).

Table 1: Main night sky emissions in the optical and near-IR (compiled from [2], [18] and [20]).

Emitter	λ (nm)	Intensity		Notes
		Night (R)	Aurora (kR)	
OI	557.7	250	100	<100 R to > 500 R night-to-night variation
OI	630.0-636.4	100	2-100	sporadic enhancements in tropical night glow
OI	777.4	-	10	
OI	844.6	-	12	
NI	346.6	-	1	ICB III Aurora
NI	519.9	-	0.1-2	ICB III Aurora
NII	VIS,FUV	-	45	
NaI	589.0-589.6			NaD, strong seasonal variation
		30	1	summer
		200	1	winter
N ₂	IR	-	880	1st positive, ICB III Aurora
N ₂	UV	-	110	1st positive, ICB III Aurora
N ₂	Blue	100	55	Vegard-Kaplan bands, ICB III Aurora
N ₂ ⁺	NUV,VIS	-	150	1st negative, ICB III Aurora
N ₂ ⁺	630-890	-	630	Meinel bands, ICB III Aurora
O ₂	300-400	1500	-	Herzberg, and Chamberlain bands
O ₂	864.5	500	60	Atmospheric bands (0-1) R and P, ICB III Aurora
O ₂ ⁺	VIS,IR	-	26	1st negative, ICB III Aurora
OH	VIS	130	-	(5-0) (7-1) (7-2) (9-3) ... bands
OH	8342	2000	-	(6-2) band
OH	Total	4.5×10^6		
NO ₂	400-700	250		nightglow pseudo-continuum
Hel	1083	-	1000	

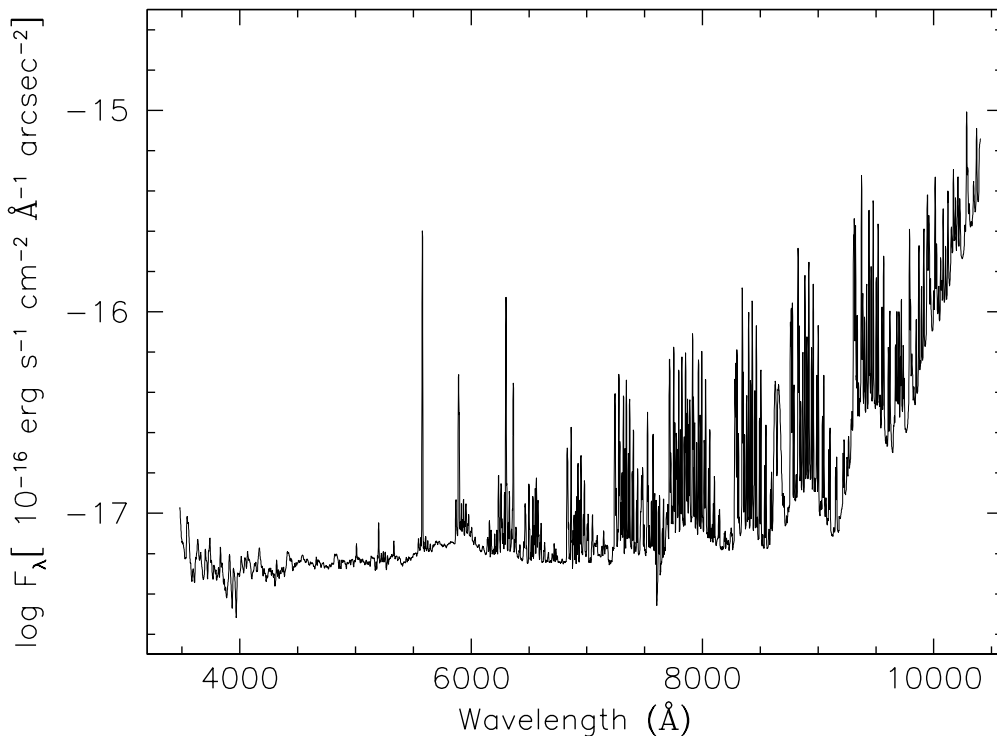


Figure 2: Optical night sky spectrum obtained at Paranal with FORS1 (resolution of $\sim 5\text{\AA}$ FWHM).

2.1 Airglow

Airglow (a.k.a. nightglow), is caused by ambient excitation (usually photochemical) of upper-atmosphere atoms and molecules (mesosphere, 85-90 km). The main parameters that govern the airglow brightness are as follows:

- geomagnetic latitude (?), season, solar activity, wavelength

A low resolution spectrum in the optical and near-IR domain is presented in Figs. 2 and 3. While the flux in the blue region ($\lambda < 5500\text{\AA}$) is produced by the so-called NO_2 pseudo-continuum, the red is totally dominated by the OH bands emission bands [2], which are also the responsables for the non-thermal emission in the IR (see for example [17]). Line atlases have been published both for the optical [9] and the IR [19]. The night sky emission is in general extremely variable even on short time scales and these fluctuations are stronger at longer wavelengths. In some passbands, like I and J, the OH bands show a steady decline in the first two hours after the end of evening twilight.

It is often mentioned in the literature that the airglow depends on the geomagnetic latitude (see for example [11], [1]). However, I could not find very precise statements, let alone direct measurements. For example, [20] states that the airglow is brighter at middle and high latitudes than at low latitudes and some emissions (like OI 6300, 6363 \AA) increase by a factor 2 [3]. At low and mid-latitudes there is a semi-annual variation in atomic hydrogen, which is in turn thought to be the responsible for the OH nightglow fluctuations [12]. At least in the optical, once one takes into account the effect of solar activity (which can give a variation of ~ 0.4 - 0.5 mag on a full solar cycle), all light pollution-free sites show very comparable night sky surface brightnesses (see [11], [13], [21]).

The lack of measurements at high latitudes is essentially due to the fact that most observatories are placed at equatorial or tropical latitudes. The few available data, however, seem to indicate

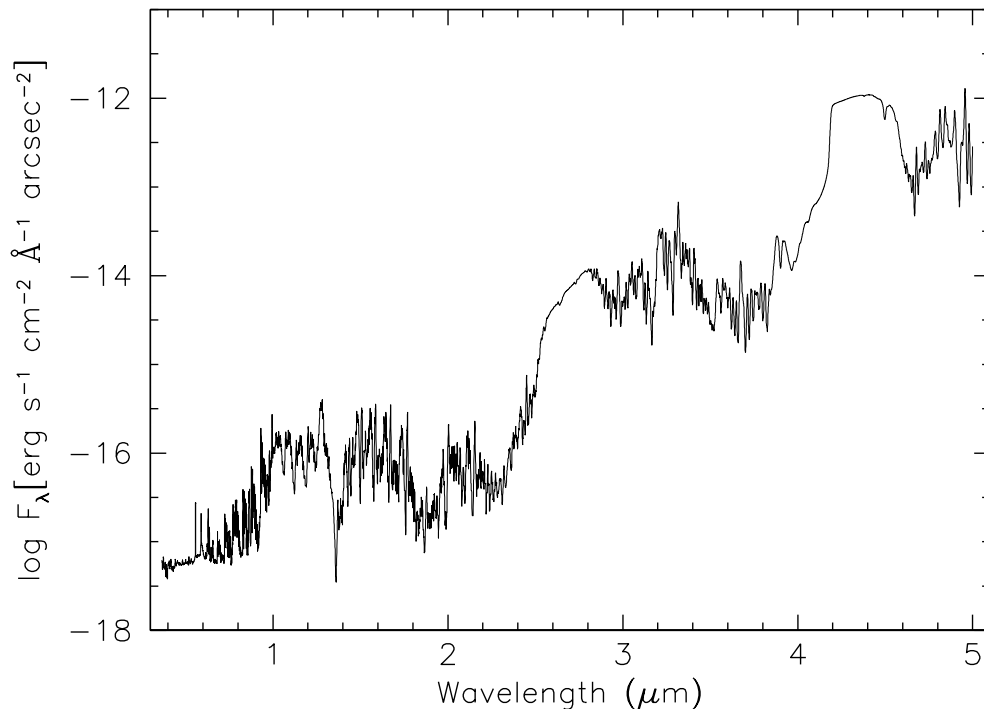


Figure 3: Optical-IR night sky spectrum. For $\lambda < 1\mu m$ the spectrum is that presented in Fig. 2 while for $\lambda > 1\mu m$ the synthetic model used in Gemini Exposure Time Calculator was adopted.

that there is no strong dependency on the geomagnetic latitude, at variance with what happens for auroral activity.

As far as the satellite observations are concerned, the data provided by the Improved Stratospheric and Mesospheric Sounder on the UARS satellite show no differences (within the errors) between high and mid-latitudes in the average intensities of OH nightglow [22]. Also, the ground-based measurements of OH emission between 837.5 nm and 856.0 nm obtained at Davis, Antarctica (68 degrees south) do not show significant differences with respect to low-latitude sites (see [10] and references therein).

The conclusion of my search in the literature is that there is no clear indication of a geomagnetic latitude dependency of the airglow, while this is more firmly established for auroral emission. In this respect, it is worth noting that two experiments are being setup at Dome C, namely *Gattini* and *Nigel* (J. Storey and A. Moore, private communication). Those instruments are going to provide spectrophotometry both during twilight and night time.

As far as the site dependency of IR background is concerned, the situation is less clear. The background at 1.7 μm on Paranal has been reported to be a factor 4 brighter than in Mauna Kea [6]. Since at this wavelength the thermal emission is still negligible (see Fig. 7), the difference is indeed difficult to explain. However, this is in conflict with the values reported by UKIRT¹, which are in good agreement with those measured at Paranal².

2.1.1 The case of NaI D lines

While all night sky emission lines are indeed hindering astronomical observations, there is one remarkable exception, namely the Sodium D lines (5890, 5896 Å), on which the whole LGS

¹See <http://www.jach.hawaii.edu/UKIRT/astronomy/sky/skies.html>

²See <http://www.eso.org/gen-fac/pubs/astclim/paranal/skybackground/>

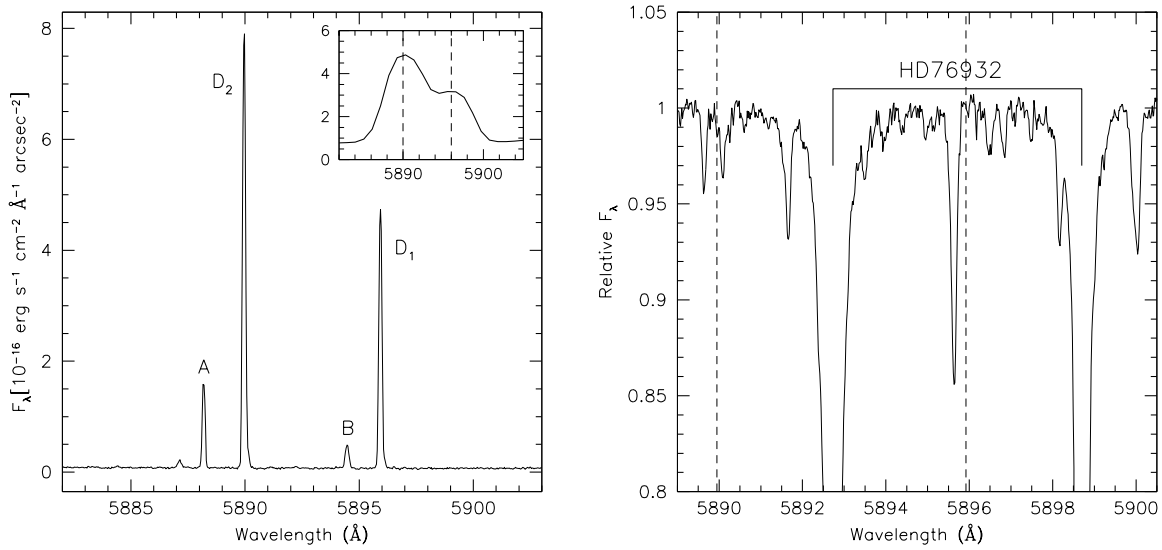


Figure 4: Left panel: Night sky UVES spectrum in the region of the NaI D lines (resolution of $\sim 0.15\text{\AA}$ FWHM; [9]). The upper insert shows the appearance of the same region in low resolution (FORS1, $\sim 5\text{\AA}$). Right panel: UVES spectrum of the bright F7 star HD 76932 ($V \sim 5.5$), courtesy of F. Primas. The vertical dashed lines mark the rest frame D lines wavelengths.

technique is based.

Monitoring of the sodium layer is usually done with a laser and provides knowledge of the sodium variability on the shortest time scales. There is also another technique, which relies on medium-high resolution spectroscopy of the sodium doublet. Due to the required exposure times this is of course not going to give information on the variations on times scales of seconds, but it can provide an alternative monitoring tool. Experiments have been done in the past in order to inter-calibrate laser measurements with spectroscopic observations [7]. The relevant spectral region is shown in the left panel of Fig. 4 (UVES, resolving power 42,000). The sodium D lines appear to be close to two of the OH (8-2) emission lines (marked as A and B). As it is shown in the upper left insert, the four lines appear to be blended at a resolution of about 1200. Nevertheless, A (5888.2\AA) and B (5894.5\AA) features account for $\sim 12\%$ of the total flux carried by the D lines. Therefore, medium resolution spectroscopy might still be a potential source of information on the sodium layer.

For the sake of completeness, we mention here the possibility of doing the same kind of analysis using the observations of the D lines *in absorption* against a bright star, as proposed in [15]. However, this method is probably going to be affected by the presence of the ubiquitous sodium lines in the stellar spectrum and in the interstellar environment and may indeed require higher resolution (and hence higher exposure times and/or large telescopes). An example is shown in the right panel of Fig. 4, where the identification of rest frame absorption D lines is actually not clear. Obviously, degrading the resolution to a few thousands would produce completely wrong results.

2.2 Aurorae

Aurorae are generated by the excitation of upper-atmosphere atoms and molecules by energetic particles, in atmospheric layer at 250-300 km. The main parameters that govern the auroral brightness are the following:

- geomagnetic latitude, season, solar activity, magnetic activity, wavelength

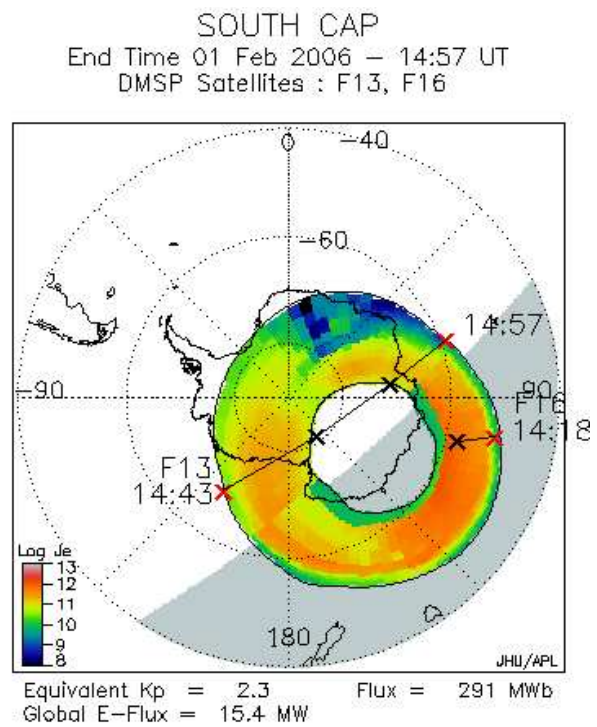
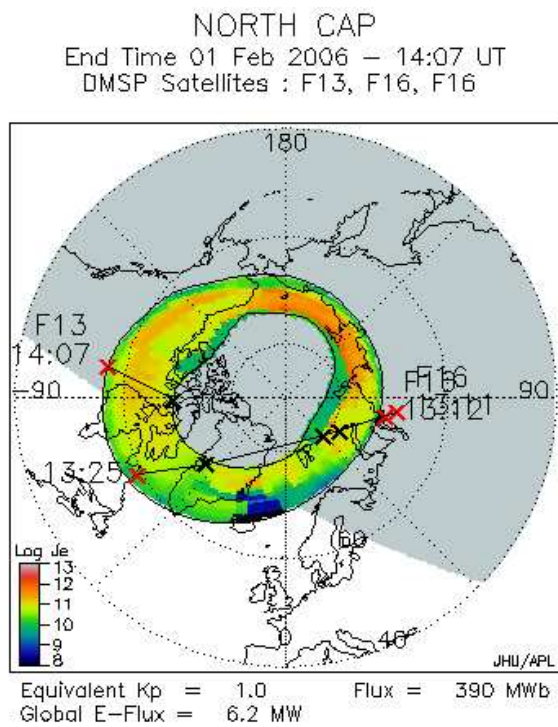


Figure 5: OVATION North (left) and South (right) polar cap plots.

2.3 Polar aurorae

Aurorae are a serious problem for ground-based astronomy only at high latitudes, within what is generally indicated as the auroral zone. This extends from 15 to 25 degrees from the geomagnetic pole, a region which is called the auroral oval. A monitoring of the auroral oval size and position is provided by OVATION (Oval Variation, Assessment, Tracking, Intensity, and Online Nowcasting)³. An example is shown in Fig. 5.

Aurorae typically take place in atmospheric layers between 100 and 250 km above the ground, with occasional peaks up to 1000 km (see for example [20]). This potential problem for high latitude sites has been analyzed and discussed in [10] in connection to the Dome C case. The conclusion is that aurorae at 100 km (or below) are not visible from Dome C, while for an height of 250 km they would be visible at elevation of about 7 degrees above the horizon and therefore would only weakly increase the night sky brightness (see also Fig. 6). Nevertheless, this conclusion must be taken with care. Direct measurements are still missing, but they will be soon provided by the two experiments previously mentioned.

2.4 Micro-auroral activity

Sites located at $\pm 20^\circ$ from the geomagnetic equator are known to show micro-auroral activities [18], with sudden variations of emission lines like [OI] 6300, 6364 Å. However, the impact in terms of night sky brightness enhancement is negligible (see for example [13]).

3 Thermal emission in the IR

At wavelengths longer than about $2 \mu\text{m}$ the atmospheric thermal emission becomes relevant (see Figs. 7 and 8). There are two windows centered at 3.5 and $10 \mu\text{m}$ where the thermal background is minimum, while maxima are reached at about 7.5 and $14 \mu\text{m}$.

³See <http://sd-www.jhuapl.edu/Aurora/ovation>

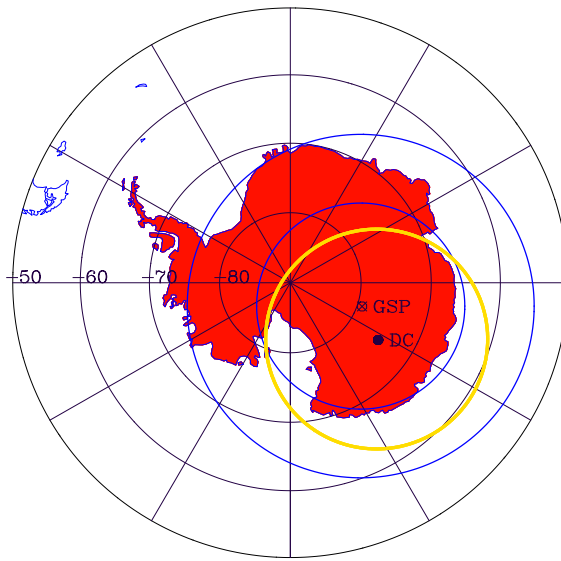


Figure 6: Schematic representation of the typical southern auroral oval, showing the geomagnetic South Pole (GSP) and Dome C (DC). The auroral oval boundaries, marked by the two blue circles, typically extends from 15 to 25 degrees from the GSP. Aurorae at 250 km altitude will be above the horizon at Dome C only if they line within the thick yellow circle (adapted from [10]).

There is a clear dependence on the site elevation, since the temperature of the lower atmospheric layers decreases very rapidly with altitude. At about 4000 m the thermal background in the window centered at $10 \mu\text{m}$ becomes almost a factor 5 weaker.

There are no clear indication about latitude dependency, while very cold sites show exceptionally low sky backgrounds, as it is the case for Dome C, both in the IR and in the sub-millimeter domain (see [10] and references therein).

4 Scattered moonlight

Scattered moonlight contributes in a dominant way to the optical night sky background when the Moon is above the horizon (at Paranal this is about 40% of the total twilight-to-twilight night time). Even though this is an unavoidable fact, different sites can show different amounts of scattered light, mainly for two reasons. The first is a different content in the aerosols, which can indeed change the impact. The other is the geographic latitude. In fact, for a given alt-az position in the sky, the background enhancement grows with the Moon height above the horizon. Therefore, at high latitude sites the moon impact is smaller than at equatorial sites, where the Moon can actually pass through zenith (see also the discussion in [10]).

The presence of scattered moonlight, which has essentially a blue spectrum peaking at 4500\AA , becomes of course progressively irrelevant as one goes into the IR domain.

4.1 Contrails

The problem of contrails is quite extensively discussed in [16]. The effects of contrails are temporary increased extinction, degradation of seeing and possible disturbs in high resolution spectra in the form of absorption lines/bands. I deem that the stronger effect comes in the form of an enhanced sky background in the presence of Moon light, as it is the case when thin/thick cirrus are present. See the discussion in [16] for more details.

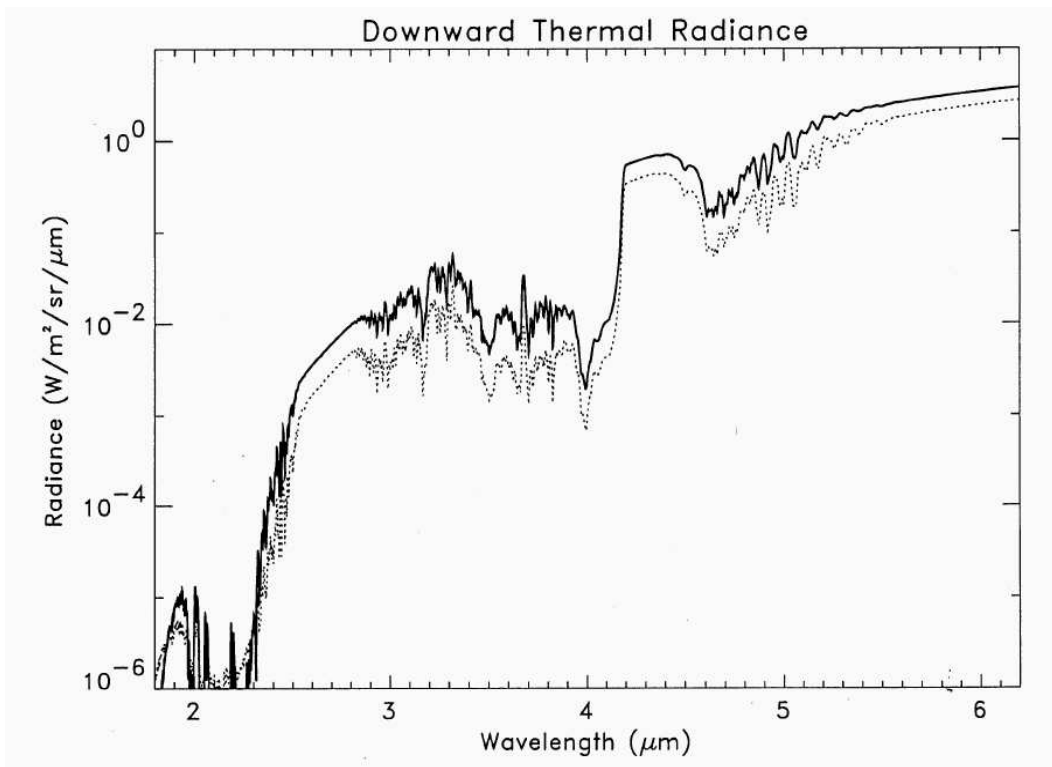


Figure 7: Downward thermal radiance in the near-IR at sea level (solid) and 4000 m a.s.l. (dotted) (from [20]).

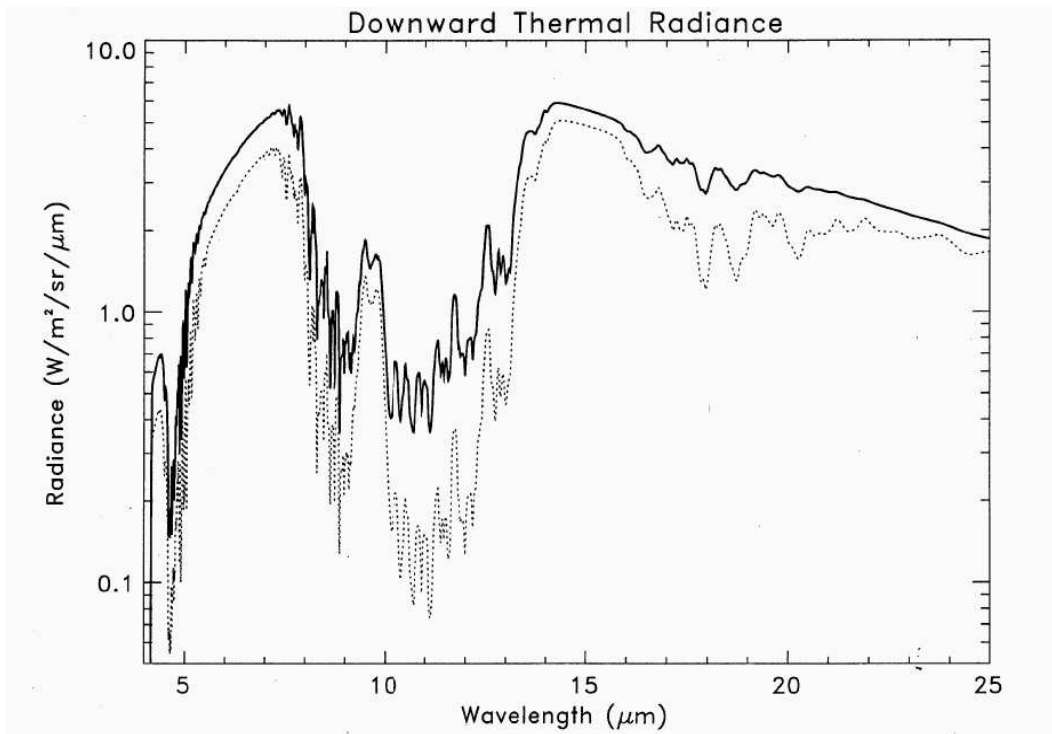


Figure 8: Downward thermal radiance in the IR at sea level (solid) and 4000 m a.s.l. (dotted) (from [20]).

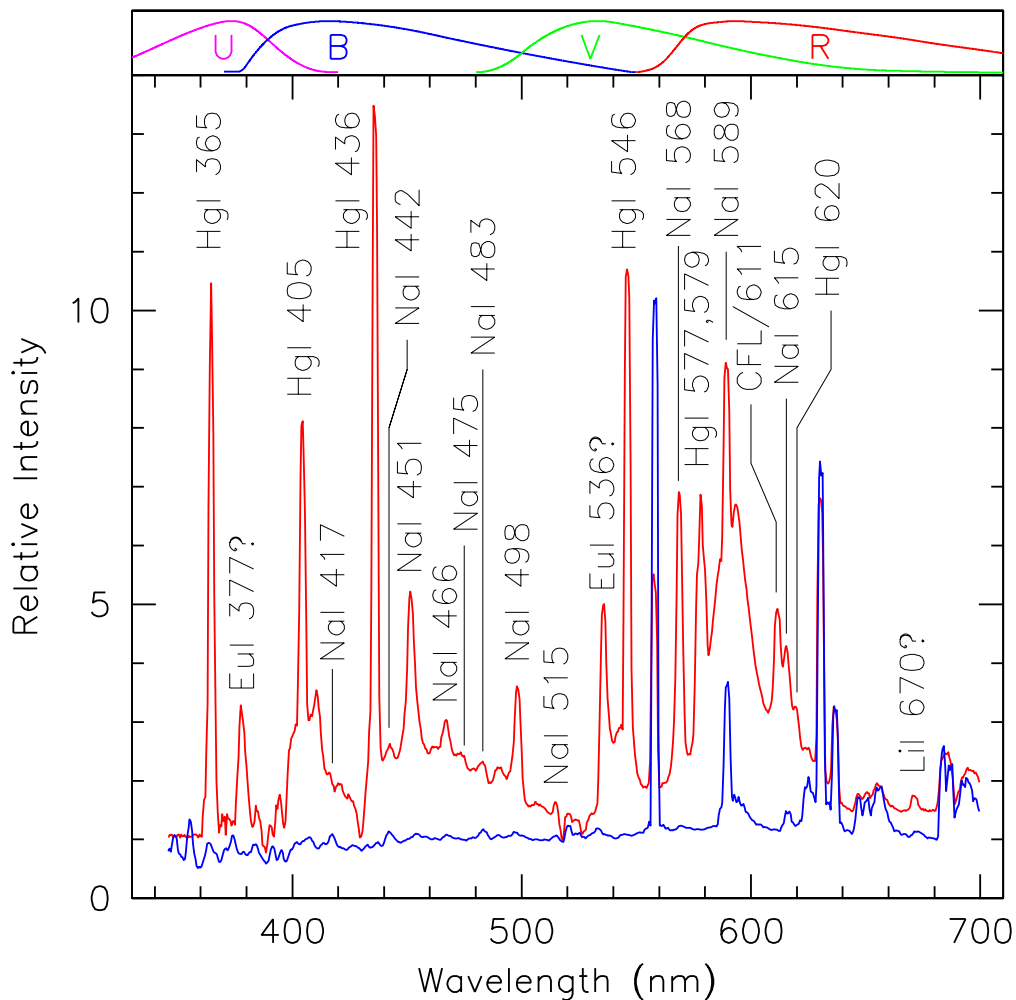


Figure 9: Comparison between night sky spectra obtained at Paranal (blue) and in a light-polluted site (red, Asiago Observatory, Italy).

5 Light Pollution

In addition to the *natural* components, human activity has added an extra source, namely the artificial light scattered by the troposphere, mostly in the form of Hg-Na emission lines in the blue-visible part of the optical spectrum (vapor lamps) and a weak continuum (incandescent lamps) [1]. With the advent and the diffusion of Compact Fluorescent Lamps, the situation has become even worse, since these lamps tend to reproduce the solar spectrum by emitting a forest of emission lines across the whole optical spectrum (see Fig. 9).

Nighttime optical images of the Earth at night have been obtained from the Defense Meteorological Satellite Program (DMSP). These data have been used to estimate the upward light flux of sources on the Earth surface and to compute the effects on the night sky modeling the light propagation in the atmosphere [4]. A world map is shown in Fig. 10.

6 Extra-terrestrial background

The extra-terrestrial background is generated by unresolved stars and galaxies and, most important, by the sun light scattered by the interplanetary dust, also known as zodiacal light. The latter contributes to about half of the brightness of the night sky in the visible, it peaks at about 4500\AA and at 8000\AA becomes only 10% of the OH airglow. At longer wavelengths, the

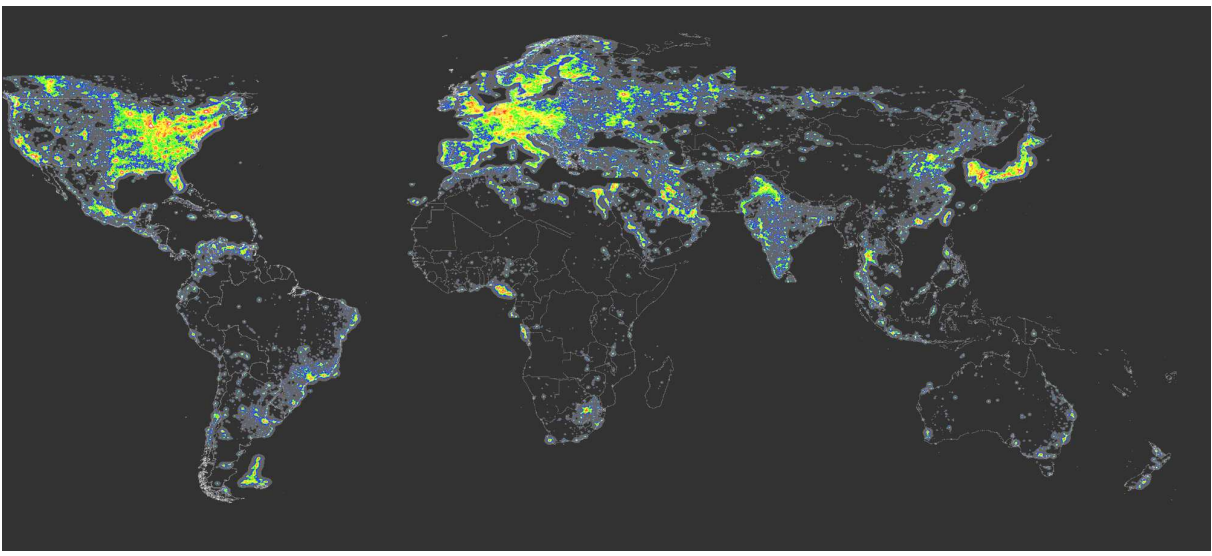


Figure 10: Artificial V sky brightness at zenith in clean nights, obtained by Cinzano et al. [4]. The mas has been computed using Garstang [8] models and measurements obtained by the Operational Linescan System of US Air Force DMSP satellites. The effects of extinction along light paths, double scattering of light from atmospheric molecules and aerosols, Earth curvature and aerosol content of the atmosphere are included.

interplanetary dust gives a contribution to the background in the form of thermal radiation, with a spectrum that peaks at about $12 \mu\text{m}$ (see [11] and references therein).

Of course the contribution depends on ecliptic latitude and helioecliptic longitude. Therefore, equatorial sites, for which the ecliptic is rather high in the sky, do show a higher zenith background than high latitude sites. Strictly speaking, this is not an intrinsic feature of the site but rather of the typical portion of the sky observable from that site. In general, when comparing different sites, the contribution of the zodiacal light has to be taken into account, as it is the case for the solar cycle phase.

Finally, the different apparent positions of the ecliptic plane during the year can mimic intrinsic seasonal variations.

7 Conclusions

- In light pollution-free sites the optical night sky brightness due to airglow is in general independent from the geographical position. Altitude is not expected to play a role in this respect. The night sky brightnesses in V at Crimean Observatory (600m), Paranal (2600m) and Mauna Kea (4200m) are comparable.
- The situation is less clear in the OH dominated near-IR region, since not many measurements at non-tropical sites are available. In principle, no difference is expected.
- In the IR the background is definitely lower in colder sites and at higher altitudes, due to the decreased thermal emission.
- Small micro-auroral effects at sites close to the geomagnetic equator do exist, but their contribution to the global background is negligible.
- Auroral activity is a serious issue for locations at high latitudes and the effects in the optical can be rather severe. The motion of the magnetic poles can cause problems in sites where this used not to be a problem.

- The contribution to the background by the extra-terrestrial component changes with the site latitude. But this is related to the different regions of the sky which are accessible from a given site rather than to the characteristic of the site itself.

8 Appendix - Measuring the sky background

One important issue with the site testing is the inclusion of sky background measurements. For obvious reasons, any instrumentation designed for this purpose has to be simple, compact, light and must operate in a fully automatic way. As far as the spectro-photometric accuracy is concerned, 10 to 15% is sufficient.

The ideal solution should be searched within commercial products, especially for what concerns telescopes, mounts and detectors⁴.

Normally, sky brightness surveys are operated using small size telescopes (0.3-0.4m) coupled to a diaphragm photoelectric photometer with broad band filters. In this case, the operator has to chose a star-free area and this makes the operation slow and not viable for automatic campaigns. Therefore it is clear that one needs panoramic detectors in order to be able, in the data reduction phase, to reject stars and other bright astronomical objects that may fall in the field of view. Algorithms specifically designed for this purpose are available (see for example [14] and references therein).

Different degrees of complexity can be considered, all including Peltier-cooled CCD detectors:

- Imaging wide field camera, at least V filter
- Imaging camera, few square deg field of view, at least V filter;
- Imaging camera, few square deg field of view, $BVRI$ filters;
- Low resolution (30-50Å) spectrograph, covering 500-1000 nm.

In the following subsections, the single cases are discussed separately.

8.1 Wide Field camera

This is probably the simplest solution. Due to the necessarily small focal length of the camera, there is most likely no need for tracking. Therefore the telescope can simply point the zenith and images can be continuously acquired and processed online by a simple automatic pipeline. The main issue with this setup is that wide field cameras are difficult to calibrate in photometric terms. Moreover, due to the necessarily big projected pixel size, stellar crowding may become too high so that measurements *in between the stars* can be difficult and/or inaccurate.

The advantage is that a great portion of the sky is covered, and this offers the chance to detect possible light pollution effects in some specific and critical directions, or to characterize the Moonlight effect as a function of all relevant parameters in one single shot.

8.2 Few square deg camera

This requires a telescope with a larger focal length and, therefore, it has to include the possibility of pointing and tracking. Pointing does not need to be accurate and so does the guiding. Even badly guided star trailings will be removed during the reduction. Given the

⁴For imaging cameras and two spectrographs see for example <http://www.sbig.com/sbwhtmls/online.htm>

pointing capability, one can think about the possibility of specifying a grid of *empty-fields* across the sky, that would allow one to get sky maps.

As far as filters are concerned, the simplest solution is to have just one, the V filter, hence reducing the weight and complexity caused by the presence of a filter-wheel. The V passband includes the bright airglow lines (and the aurora lines) and also the bright light pollution Hg and Na lines. On the other hand it does not include the OH lines. For this a R or better I filter would be required.

8.3 Long slit - low resolution spectrograph

Considering the fact that portable IR instrumentation is not a viable solution, the top setup for sky brightness measurements is a low resolution spectrograph that covers the region 500-1000 nm, i.e. giving a full coverage of airglow, aurora, light pollution and OH optical features. At a resolution of 50\AA the most important features would be visible (see Fig. 11) and would allow studies of seasonal/latitudinal trends of micro-auroral, auroral and OH features (for NaID studies the resolution is far too low).

There is a main problem with this, i.e. the fact that one necessarily needs to have a slit and this has to be placed in reasonably star free areas. This problem can be mitigated by a smart data processing coupled to the long slit, in the sense that one can reasonably assume that most of the pixels will be dominated by sky background.

The instrument has to be kept very compact in order to be mounted on a small telescope. An example is given in [5], even though that instrument was designed for light polluted sites, i.e. with a much brighter background.

A possible alternative is a fiber-fed spectrograph. This would greatly reduce the weight, but it would introduce the problem that during the data processing is impossible to disentangle the contribution of the background from that of possible astronomical objects falling into the fiber.

In all cases wavelength calibration is not an issue, since the night sky lines themselves can be used. As for the flux calibration, bright standard stars for professional instruments can be easily observed once in a while to get reference sensitivity curves.

For what concerns data processing, there is no major problem. The only real issue for the absolute fluxing is the stability of bias level and dark current. In the case of Peltier-cooled detectors this might require the need of taking calibration frames during the measuring sessions. Of course, this problem affects both imaging and spectroscopy. If the controller allows for pre/over-scan readings, this issue becomes much less important.

I believe that, in general, for imaging one can easily find all required hardware on the market. For the spectrographs there is not much available. Nevertheless, current commercial solutions should be considered. For example, the SBIG DSS-7 spectrograph covers the range 400-800 nm (see Fig. 12 for an example night sky spectra obtained with this instrument). This is a very compact and low weight instrument (~ 1.1 kg) and the price is around 1500 USD. The dispersion is $5\text{\AA}/\text{pix}$ and resolution is about 15\AA ($7\ \mu\text{m}$ px, ST-7 camera). Testing is of course required, but I think that such a setup would be already sufficient for our purposes.

Things get of course extremely more complicated in the case of site testing in extreme conditions, like in Antarctica. On the other hand, this site is quite unique and site testing campaigns are already in place and they should provide us with the relevant data in due time.

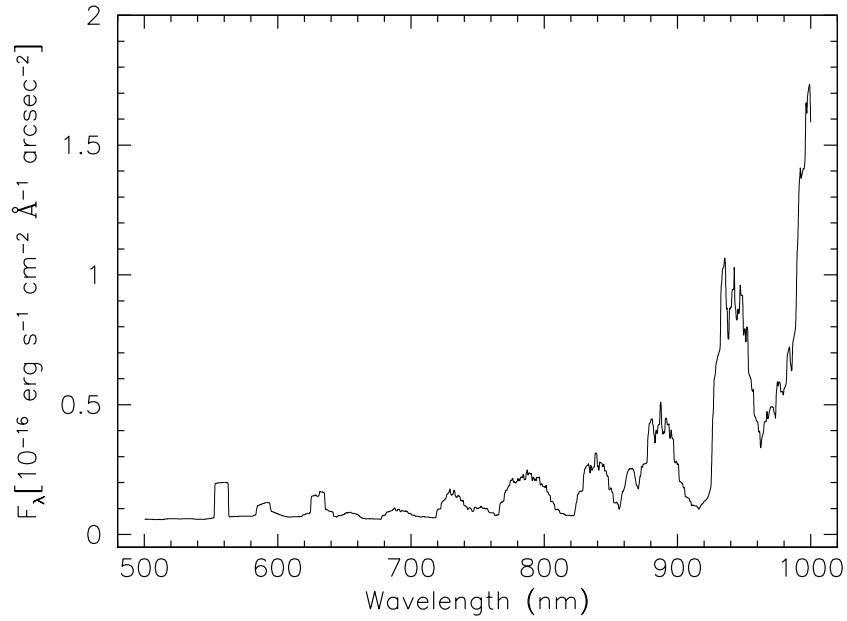


Figure 11: Optical night sky spectrum in the region 500-1000nm degraded to a resolution of 50 Å.

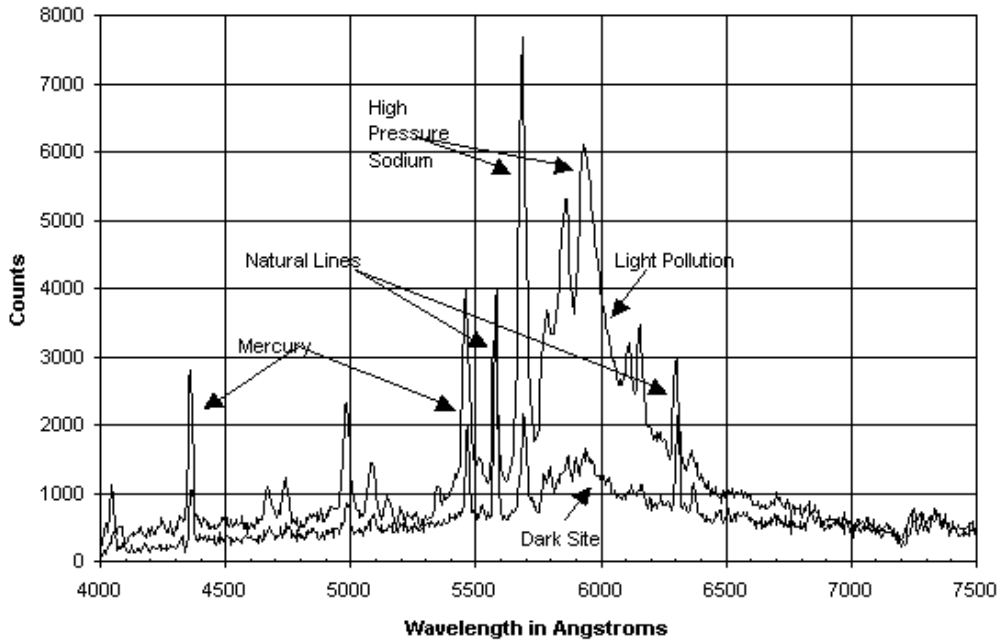


Figure 12: Optical night sky spectra obtained at two different sites with the SBIG DSS7 spectrograph (from the SBIG web site). Note that what is called here *dark site* shows clear signs of light pollution (compare with Paranal spectra).

References

- [1] Benn, C.R. & Ellisson, S.L., 1998, Atmospheric extinction at the Roque de los Muchachos Observatory, La Palma Tech. Note n. 115
- [2] Broadfoot, A.L. & Kendall, K.R., 1968, *J. Geophys. Res.*, 73, 426
- [3] Chamberlain, J.W., 1961, *Physics of the Aurora and Airglow*, (Academic Press: New York)
- [4] Cinzano, P., Falchi, F., Elvidge C.D. 2001, The first world atlas of the artificial night sky brightness, *MNRAS*, 328, 689
- [5] Cinzano, P., 2004, A portable spectrophotometer for light pollution measurements, *Mem. S.A.It. Suppl. Vol. 5*, 395
- [6] Cuby, J.G., Lidman, C. & Motou, C., 2000, ISAAC: 18 months of Paranal Science Operations *The ESO Messenger*, 101, 2
- [7] d'Orgeville, C. et al., 2003, Preliminary results of the 2001-2002 Gemini sodium monitoring campaign at Cerro Tololo, Chile, *SPIE*, 4839, 492D
- [8] Garstang, R.H., 1989, Night sky brightness at observatories and sites, *PASP*, 101, 306
- [9] Hanuschik, R., 2003, A flux calibrated, high resolution atlas of optical sky emission from UVES, *A&A*, 407, 1157
- [10] Kenyon, S.L. & Storey, J.W.V., A review of optical sky brightness and extinction at Dome C-Antarctica, 2005, *PASP*, in press, astro-ph/0511510
- [11] Leinert, Ch. et al., 1998, The 1997 reference of diffuse night sky brightness, *A&ASS*, 127, 1
- [12] Le Texier, H., Solomon, S. & Garcia, R.R., 1987, Seasonal variability of the OH Meinel bands, *Planet. Space Sci.*, 35, 977
- [13] Patat, F., 2003a, UBVRI night sky brightness at sunspot maximum at ESO-Paranal, *A&A*, 400, 1183
- [14] Patat, F., 2003b, A robust algorithm for sky background computation in CCD images, *A&A*, 401, 797
- [15] Patriarchi, P. & Cacciani, A., 2000, Monitoring of the mesospheric sodium layer using a magneto-optical filter, *SPIE*, 4007, 368
- [16] Pedersen, H., 1998, VLT observing conditions monitor, ESO internal document
- [17] Ramsay, S.K., Mountain, C.M. & Geballe, T.R., 1992, Non-thermal emission in the atmosphere above Mauna Kea *PASP*, 259, 751
- [18] Roach, F.E. & Gordon, J.L., 1973, *The light of the night sky*, Dordrecht-Reidel
- [19] Rousselot, P., Lidman, C., Cuby, J.G., Moreels, G. & Monnet, G., 2000, Night-sky spectral atlas of OH emission lines in the near-IR, *A&A*, 354, 1134
- [20] Schubert, G. & Walterscheid, R.L., 2000, Earth, in *Allen's Astrophysical Quantities*, ed. A. Cox (New York: AIP Press; Springer), 4th edition, 239

- [21] Walker, A. & Schwarz, H.E., 2005, Night Sky Brightness at Cerro Pachon, http://www.ctio.noao.edu/site/pachon_sky
- [22] Zaragoza, G., Taylor, F.W. & Lopez-Puertas, M., 2001, Latitudinal and longitudinal behaviour of the mesospheric OH nightglow as observed by UARS/ISAMS J. Geophys. Res., 106, 8027